Journal of Fluids and Structures (2001) **15,** 617–628
doi:10.1006/jfls.2000.0361, available online at http://www.idealibrary.com on IDEAL®

THE SUPPRESSION OF LIFT ON A CIRCULAR CYLINDER DUE TO VORTEX SHEDDING AT MODERATE REYNOLDS NUMBERS

C. DALTON, Y. XU

Mechanical Engineering Department, University of Houston
Houston, TX 77204-4792, U.S.A.

AND

J. C. OWEN
Department of Aeronautics, Imperial College
London, SW7 2BY, U.K.

(Received 11 August 2000, and in final form 14 November 2000)

This paper discusses the effect of a small control cylinder on the transverse force (lift) on a large primary cylinder when the control cylinder is placed at select locations in the shear layer emanating from the primary cylinder. We have conducted both CFD and flow-visualization studies of this situation for Reynolds numbers of 100, 1000, and 3000. A 2-D Large Eddy Simulation was used in the CFD study to include the effects of wake turbulence. The CFD results show that the LES model predicts essentially an elimination of the transverse force on the primary cylinder for an appropriate placement of the control cylinder. The results also show that the drag on the primary cylinder is reduced. Our results, both from computation and flow visualization, indicate that the placement of a control cylinder has a noticeable influence on the drag and lift on the primary cylinder.

1. INTRODUCTION

VORTEX SHEDDING from bluff bodies is a recognized phenomenon since the days of Leonardo da Vinci. One effect on, say, a circular cylinder is to cause the instantaneous force acting on the cylinder to vary, with time, which can cause vibration of the cylinder. This vortex-induced vibration (VIV) is the cause of at least three troublesome situations: fatigue of the cylinder due to sustained oscillations, possible impact with adjacent cylinders due to VIV, and possible extreme buffeting of trailing cylinders due to shed vortices from the upstream cylinder.

There are several ideas that have been pursued to influence, either to minimize or eliminate, vortex shedding and, thus, to control the effects of vortex shedding. These ideas fall into either of two categories: active control and passive control. We will discuss only the passive-control devices in this paper.

Zdravkovich (1997) presents a discussion of several of the passive control devices: the perforated shroud which has the effect of influencing the base pressure; a splitter plate which prevents communication between the opposing sides of the wake; and helical strakes which have the effect of destroying the longitudinal coherence in the vortex shedding.

A fourth passive control device is the placement of a second, and smaller, cylinder in the wake of a large cylinder, which will be the focus of this study. The smaller cylinder (the

0889–9746/01/040617 + 12 $35.00/0

control cylinder) has the effect of influencing the rollup of the shear layer from one side of the larger cylinder (the primary cylinder), i.e., the side of the primary cylinder near which the control cylinder is placed. Several authors have discussed this concept from both experimental and numerical points of view. Experimentally, this problem has been studied by Sakamoto *et al.* (1991), who used a square prism as the primary cylinder. They found that a close proximity configuration led to significant reductions of the fluctuating lift and drag on the primary cylinder. Igarishi & Tsutsui (1991) used a control cylinder to reduce the drag and lift on their primary cylinder. They explained their results by saying that the control cylinder provided a turbulent jet that attached itself to the near side of the wake of the primary cylinder and prevented the traditional vortex-shedding pattern from developing. Sakamoto & Hanui (1994) studied numerous different configurations of primary and control cylinders at a Reynolds number (Re) of $6{\cdot}5 \times 10^4$. Their experimental results showed that the maximum reduction of the drag and lift occurred when the control cylinder was placed at 120° from the stagnation point. Strykowski & Sreenivasan (1990) did both an experimental and numerical study of this same problem for $\mathrm{Re} = 100$, which is in the range of a 2-D flow. They found that the control cylinder had a strong influence of the drag and lift on the primary cylinder. They attributed the drag and lift reductions to the control cylinder diffusing concentrated vorticity and a small amount of fluid into the wake of the primary cylinder where the flow was influenced by removing some of the unsteadiness from the wake.

2. ANALYSIS

We will treat the flow as 2-D and take the fluid to be incompressible. The governing equations will be expressed in general coordinates. We will spatially filter the governing equations to represent the problem by means of the Large Eddy Simulation (LES) method. Thus, the governing equations represent the 2-D resolved velocity field with the subgrid scale (SGS) effects represented by the Smagorinsky (1963) model. We use the LES method, which is normally used for 3-D representations of flow, in a 2-D simulation because of the complexities of representing two cylinders in the flow field. A full 3-D calculation would present computational requirements that would be insurmountable in terms of the facilities available to us for this study. We recognize that the 2-D calculations will not be truly representative of the actual flow at these Reynolds numbers, but the 2-D CFD analysis from this study will provide some insight not previously available. Because this is a 2-D study, we expect, based on our experience and that of others in related studies, that the calculated drag and lift coefficients will be slightly greater than the values that would have been obtained in a 3-D study.

We will use represent the problem in general coordinates and use the 3-D LES approach presented by Lu *et al.* (1997), although, in this case, we have a 2-D problem. The value for the Smagorinsky modeling constant for this problem is 0·1.

The boundary conditions to be applied are the typical no-slip and no-penetration conditions applied to the surface of the cylinders. The inflow boundary condition is that the incoming flow is uniform. The outflow boundary condition is that the flow crossing the outflow boundary is not affected by the presence of the boundary. This means that vortices approaching the outflow boundary cross the outflow boundary undisturbed by the presence of the boundary, i.e., the outflow vorticity gradients are set to zero.

3. REPRESENTATION OF A PAIR OF CYLINDERS

Representing a pair of cylinders in a flow field requires some special consideration of the geometry. Two cylinders present the problem of dealing with two branch cuts in

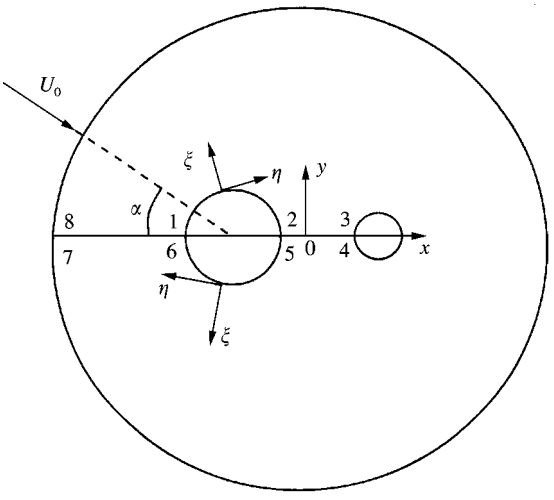

Figure 1. Schematic diagram of two cylinders.

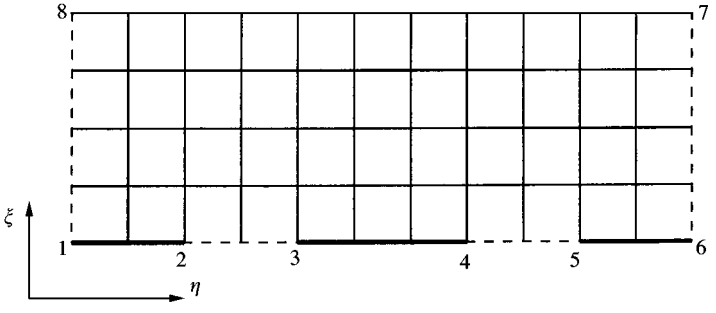

Figure 2. The two cylinders in the transformed plane.

the representation. Figure 1 shows the configuration of the cylinders in the physical plane. The branch cuts are along the lines 8–1 (or 7–6) and 2–3 (or 5–4). We need to transform the cylinders in the physical plane into a rectangular computational plane. To represent the computational plane, the region is opened as shown in Figure 2. Lines 1–2 and 5–6 represent the cylinder to the left while the cylinder to the right is represented by line 3–4. Thus, the computational grid is now rectangular which facilitates the solution of the problem. The no-slip boundary conditions for the surfaces of the cylinders are represented along the lines 1–2 and 5–6 for the left cylinder and along the line 3–4 for the right cylinder. The inflow boundary condition is represented on the ends of the line 7–8, while the outflow boundary conditions are represented toward the central part of line 7–8. The distinction between the two regions along line 7–8 cannot be specified in advance; it develops as a part of the solution. The lines 2–3 and 4–5 do not have boundary conditions specified, except to say that the values from 2–3 are the same as from 4–5. The same is said for lines 1–8 and 6–7.

4. CYLINDERS OF UNEQUAL SIZE: SUPPRESSION OF VORTEX SHEDDING

We now examine the problem mentioned in the Introduction: a primary (larger) cylinder and a control (smaller) cylinder, configured so that the control cylinder is in the vicinity of

one of the separated shear layers from the primary cylinder. Our focus in this study is to examine the effect of the control cylinder on vortex shedding of the primary cylinder, i.e., under what circumstances, if any, is vortex shedding suppressed by the control cylinder? The primary cylinder is to have a diameter 10 times that of the control cylinder, $D/d = 10$, where D is the diameter of the primary cylinder and d is the diameter of the control cylinder. We treat this problem by placing both cylinders on the x-axis and changing the angle of attack of the flow, as shown in Figure 1. In this way, we can change the position of the control cylinder relative to the separated shear layer by changing the angle of attack. Results for three different Reynolds numbers will be presented. The reference velocity in the drag and lift coefficient definitions for the control cylinder is the approach velocity to the primary cylinder. The code used for the velocity and force calculations has been thoroughly tested for a large number of cases.

4.1. RE = 100

This case is a physically 2-D, purely viscous flow calculation. The results for the drag and lift coefficients, C_D and C_L, on the primary cylinder are shown in Figure 3 for five different angles of attack at a gap distance of $R/D = 1{\cdot}4$, where R is the center-to-center distance between the two cylinders. (The term "angle of attack" used herein means the angle above the rear centerline of the primary cylinder to the location of the control cylinder.) These results show that conventional vortex shedding is essentially suppressed at 25° and 30°, i.e., the lift coefficient on the primary cylinder has become virtually a constant (although nonzero) value. The explanation for the suppression of conventional vortex shedding is that the near wake has become fairly steady in its behavior as fluid from the control-cylinder-side shear layer is drawn steadily into the wake. There is still a conventional wake present, but it has been pushed much further downstream and does not seem to be affecting the near wake. For angles of attack greater than about 30°, the control cylinder is essentially out of the wake of the primary cylinder and its effect is still present, but is lessened. The lift coefficient is oscillating with a nonzero mean value, which indicates that vortex shedding is occurring, but in a different manner than for a single cylinder. The nonzero mean value of

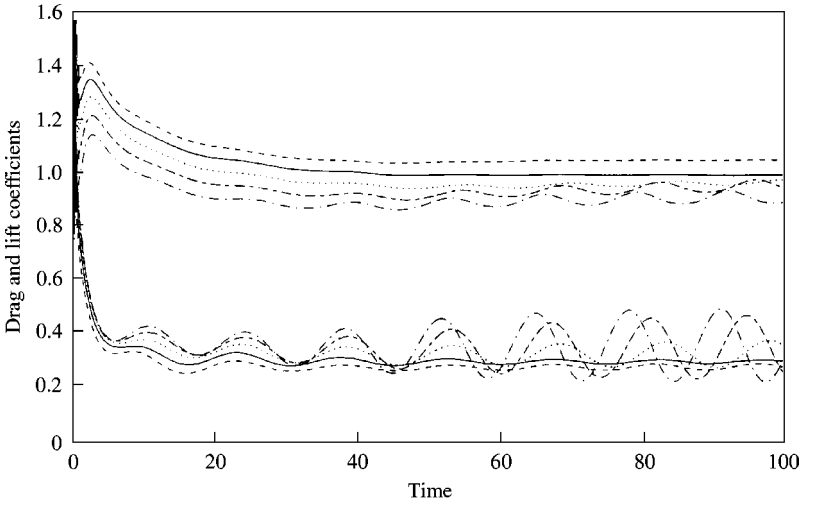

Figure 3. Drag and lift coefficients for the primary cylinder at Re = 100 and $R/D = 1{\cdot}4$: – – –, $\alpha = 25°$; ——, $\alpha = 30°$; ····, $\alpha = 35°$; – – –, $\alpha = 40°$; – · –, $\alpha = 45°$.

the lift coefficient is because the mean flow field is no longer symmetric due to the presence of the control cylinder.

Suppression of conventional vortex shedding has also affected the drag coefficient, which is seen to have a fairly flat value at 25 and 30°. The drag coefficient for a single cylinder at this Reynolds number is approximately 1·5, so not only has the lift become a constant value, the drag has also decreased in value by about 33%. Virtually no difference is observed in the drag coefficient, while the lift coefficient has decreased in value very slightly when the gap spacing is changed from 1·4 to 1·6 (results not shown).

A reason for this suppression of vortex shedding was offered by Strykowski & Sreenivasan (1990) who suggested that the "secondary (control) cylinder has the effect of altering the local stability of the flow by smearing and diffusing concentrated vorticity in the shear layers behind the body". They also noted that the control cylinder diverted a small amount of fluid into the wake of the primary cylinder. Both of these effects are seen in Figure 4 which is a plot of the vorticity field at 30° and a gap spacing of 1·4*D*. The control cylinder is quite clearly deflecting fluid into the wake of the primary cylinder. The far wake of the pair of cylinders consists of elongated and attached vortices with a much less pronounced waviness between the sides of opposing vorticity than is seen in a comparable flow without the control cylinder. The wake of the control cylinder is behaving in the same way as the wake of the primary cylinder in that there is no vortex formation and shedding occurring.

Figure 5 shows a flow visualization comparison between the cases of a control cylinder and no control cylinder at Re = 100. The control cylinder is at 30° and a gap spacing of 1·4. The near-wake behind the primary cylinder in the presence of a control cylinder is very steady compared to the case of no control cylinder. The unsteady wake seems to have been pushed farther downstream when the control cylinder is present. The steady near-wake is consistent with the calculated result of small, but steady, lift coefficient. The flow visualization technique is "laser-induced fluorescence", in which a laser sheet is used to illuminate a fluorescent dye that is washed from the front face of the cylinder as it is towed at constant velocity through water.

4.2. $\mathrm{Re} = 1000$

As stated earlier, the LES calculations for the turbulent wake cases will be 2-D because of the computational requirements to do the full 3-D two-cylinder case. We recognize the limitation of this approach, but we still feel that the results will be of practical use in examining the effects of the control cylinder. We do anticipate that the 2-D calculations will produce drag and lift coefficient values, which will be approximately 5–10% higher than would be obtained from a full 3-D simulation or from experimental results.

Figure 6 shows the drag and lift coefficient behavior for the primary cylinder for several cases. We note first that the results at Re = 1000 are noticeably more sensitive to both angle of attack of the configuration and the gap spacing. There is very little difference in both drag and lift when the angle is changed from 25 to 28°. However, when the gap spacing is increased from 1·2 to 1·6 at an angle of 25°, a conventional vortex-shedding-type behavior is present. This is explained by the control cylinder having moved to the outer portion of the shear layer where its position seems to be much less influential on the vorticity field. At an angle of 30° and a gap spacing of 1·3, the drag has decreased very slightly compared to the 25°–1·2 case, and the lift has increased very slightly with a small oscillation now present. This indicates the return of a vortex-shedding-type behavior, although it clearly is not the conventional vortex-shedding behavior expected for a single cylinder. We also note in Figure 6 that the drag coefficients at a gap spacing of 1·2 have essentially a constant value of

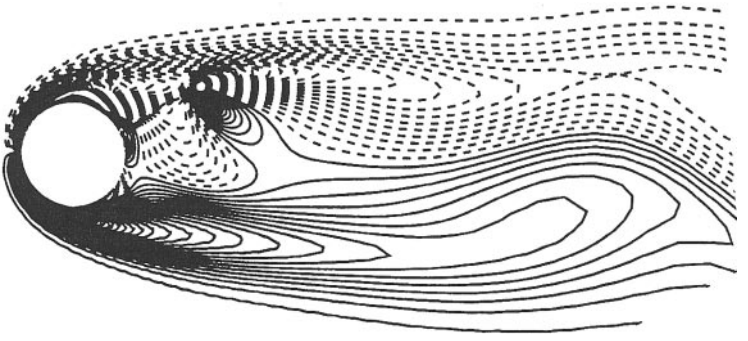

Figure 4. Axial vorticity field at Re = 100, $R/D = 1{\cdot}4$, and $\alpha = 30^{\circ}$.

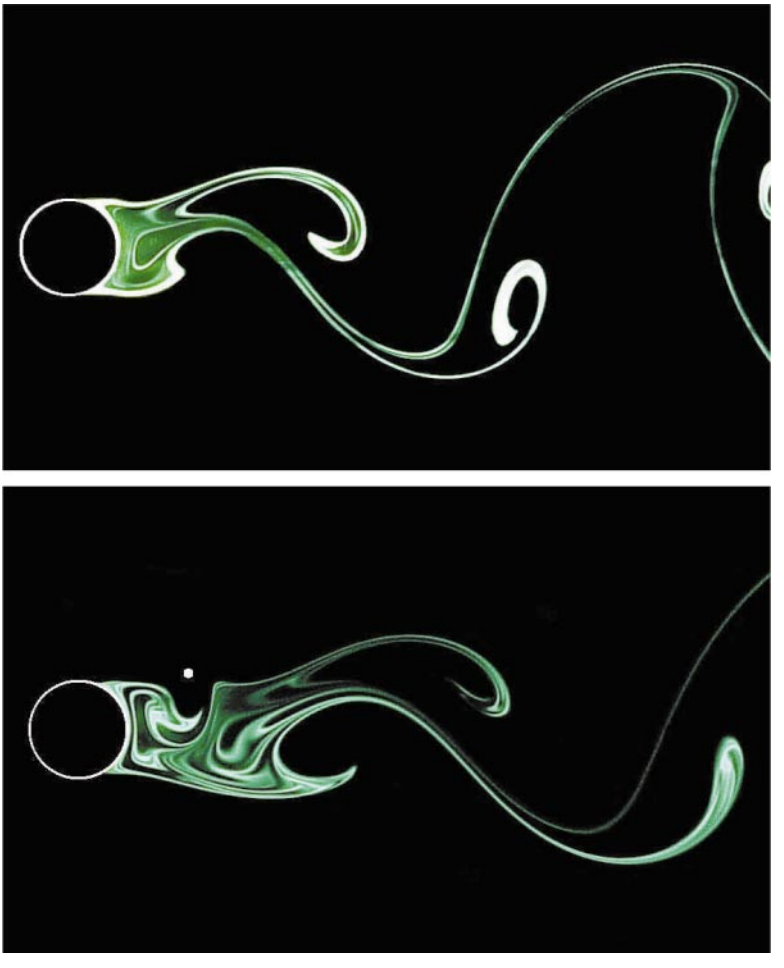

Figure 5. Flow visualization comparison at Re = 100, $\alpha = 30^{\circ}$, and $R/D = 1{\cdot}4$.

about 0·8 while the single-cylinder experimental value at Re = 1000 is about 1·0. The lift coefficient on the primary cylinder for the gap spacing of 1·2 has decreased to an almost constant value of 0·1. The lift coefficient has a nonzero mean value because the presence of

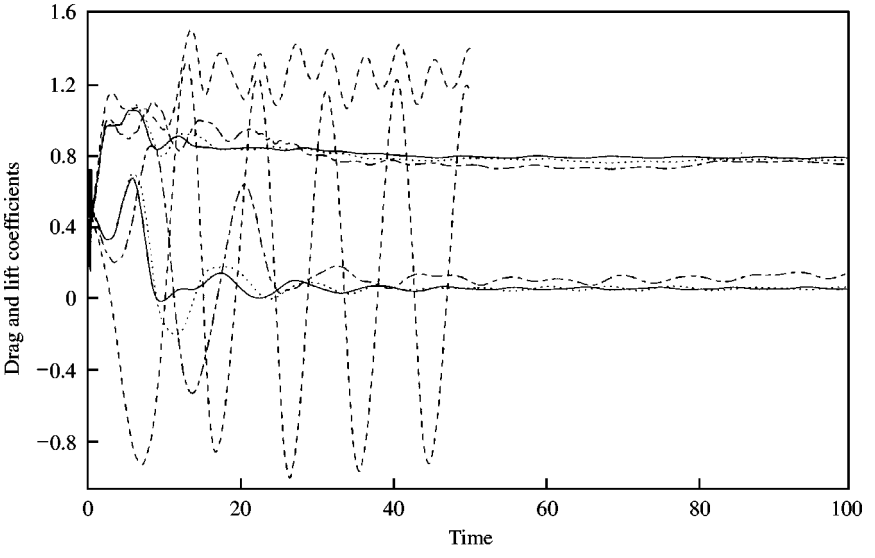

Figure 6. Drag and lift coefficients for the primary cylinder at Re = 1000 for several conditions: ——, $\alpha = 25°$; $R/D = 1{\cdot}2$; – – –, $\alpha = 25°$; $R/D = 1{\cdot}6$; ····, $\alpha = 28°$; $R/D = 1{\cdot}2$; – - – -, $\alpha = 30°$; $R/D = 1{\cdot}3$.

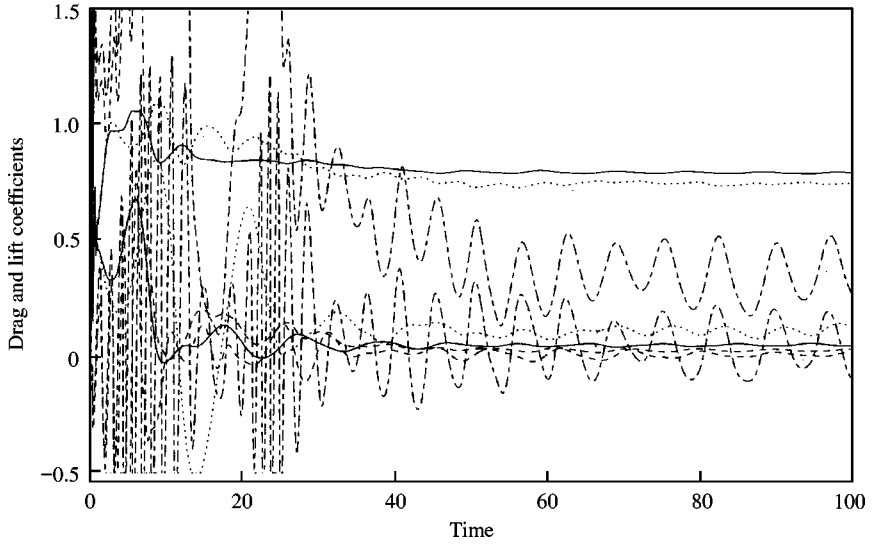

Figure 7. Drag and lift coefficients for both cylinders at Re = 1000, $R/D = 1{\cdot}2$, and $\alpha = 25°, 30°$. For $\alpha = 25°$; —, primary; – – –, control. For $\alpha = 30°$; ····, primary; – - –, control.

the control cylinder, although suppressing conventional vortex shedding, is still creating an asymmetry in the flow field.

Figure 7 shows the drag and lift coefficients for both cylinders at a gap spacing of 1·2 and two different angles of attack: 25 and 30°. The drag coefficient traces for the primary cylinder are reasonably flat at both angles, with the 30° result, at a fairly steady value of 0·8, being very slightly lower than the 25° result. Also for the primary cylinder, the lift coefficient for the 25° angle, with a steady value of about 0·1, is slightly less than the average value at 30° which also has some small-amplitude oscillatory behavior. For the control cylinder at

25°, both the drag and lift coefficients have a similar behavior; they both oscillate between 0 and 0·1. At 30°, the control cylinder has a drag coefficient with a value of about 0·35 $\pm$ 0·2 while its lift coefficient is about 0·1 $\pm$ 0·2. Based on the values of the lift and drag coefficients on the primary cylinder, these results indicate that the angle of attack position of 25° is only slightly better than the one at 30°.

The differences in drag and lift behavior noted in Figure 7 can be explained by noting the difference in wake vorticity behavior at the time the attached vortex on the primary cylinder extends farthest downstream. The vorticity plot for an angle of attack at 25° and a gap spacing of 1·2 is shown in the top part of Figure 8. First, we note that the primary cylinder wake is elongated over the wake for an isolated single cylinder. The slight oscillatory lift behavior shown in Figure 7 at an angle of attack of 25° is explained by noting, in Figure 8, the far wake of the configuration. There is a distinct Karman vortex street forming as the vortices move away from the vicinity of the cylinder pair. The near-wake at 25° shows the wake of the control cylinder is deflected down into the core of the primary cylinder wake. For the conditions shown in Figure 7, the control-cylinder wake acts as a jet-like stream that seems to steady the wake of the primary cylinder. The bottom part of Figure 8 shows the result of the same calculation for an angle of attack of 30°. The jet-like behavior seems less intense in this case. The drag and lift traces on the control cylinder at 30° show that there is time dependence in the wake behavior that is not present for the 25° case. Also, the length of the primary cylinder large vortex is greater in the 25° case which pushes whatever unsteadiness is present farther away from the near-wake. This greater wake length has the effect of steadying the near-wake and suppressing conventional vortex shedding.

Figure 9 shows a sequence of flow visualization pictures at Re = 1000, with and without the control cylinder, at the same relative time in the shedding cycle of the primary cylinder alone. The control cylinder is at 25° and a gap spacing of 1·2. In this case, the physical wake behind the primary cylinder is 3-D and turbulent which means that the flow structure from flow visualization is not nearly as vivid as at Re = 100. However, the difference in the two wake structures is still obvious. The case on the left, with no control cylinder, shows the roll-up of the vortex sheets emanating from the separation points and the alternate and

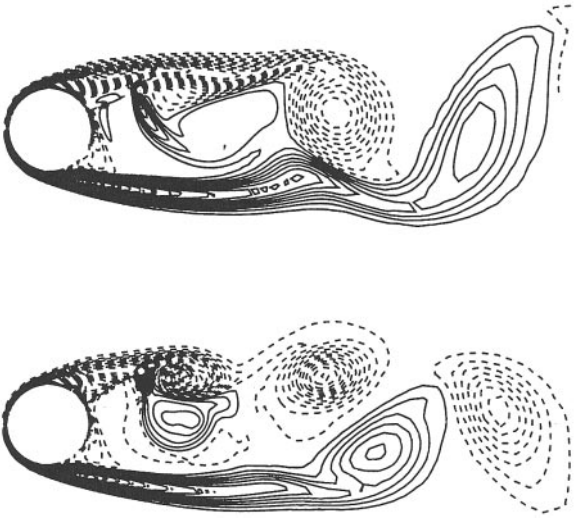

Figure 8. Axial vorticity field at Re = 1000, R/D = 1·2, and α = 25° (top). Axial vorticity field at Re = 1000, R/D = 1·2, and α = 30° (bottom).

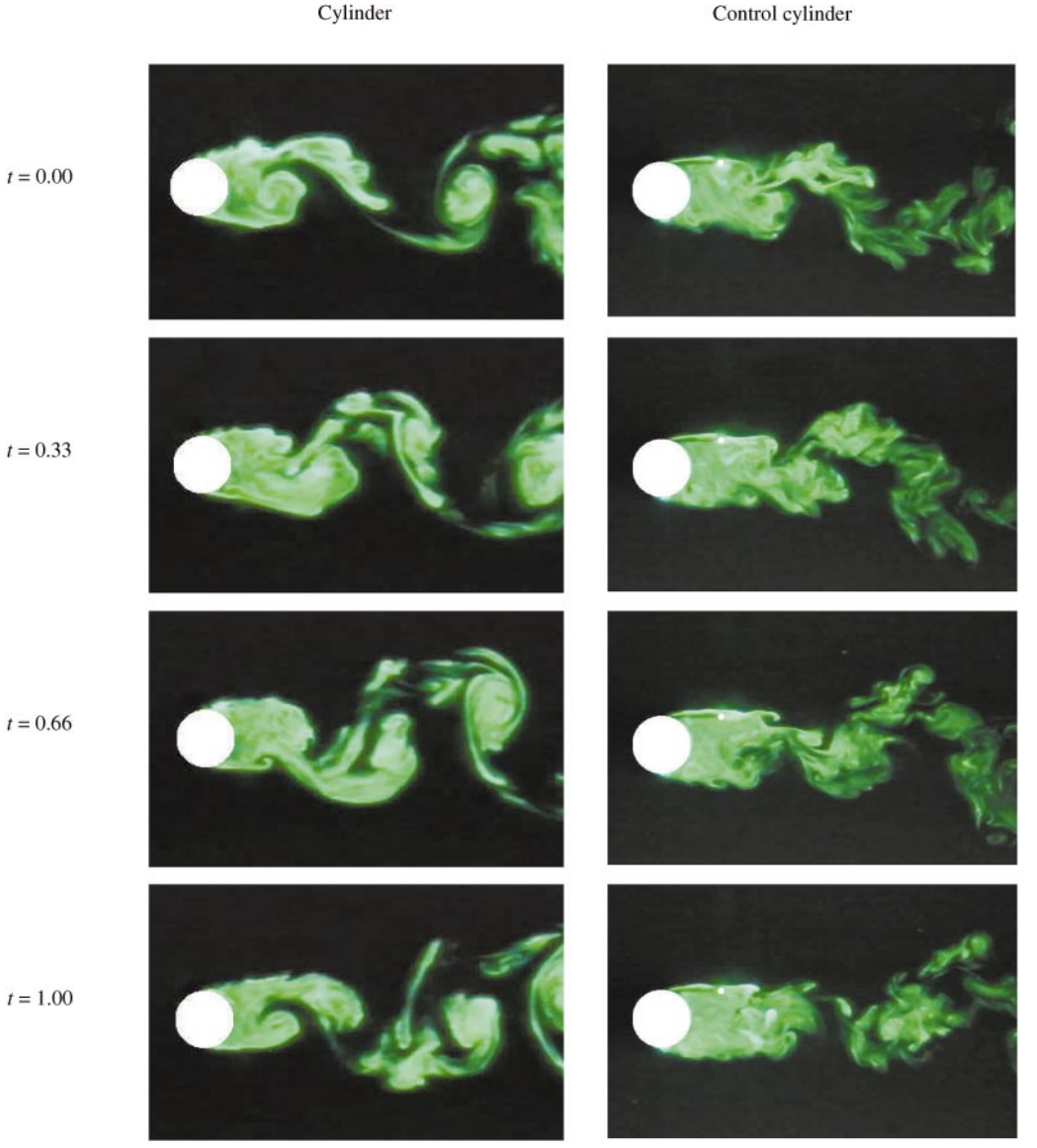

Figure 9. Flow visualization comparison at Re = 1000, $\alpha = 25^\circ$, and $R/D = 1{\cdot}2$.

periodic shedding of vortices, all of which is predictable and expected. However, the case on the right, with the control cylinder present, has a distinctly different structure. There is a shedding-like behavior, but it is less wavy and occurs slightly farther downstream. The near-wake seems to be less time-dependent. This, however, is a qualitative judgement since the turbulence in the wake distorts the mean flow structure that is present. Nevertheless, the near-wake with a control cylinder present is clearly less time-dependent which helps to explain the small, yet constant, value of the lift coefficient.

4.3. $\mathrm{Re} = 3000$

Again, this flow is at a Reynolds number at which the wake has an established turbulent behavior. However, we continue with our 2-D representation due to the computational requirements necessary to do the full 3-D two-cylinder case, fully recognizing the limitations of the 2-D results. Due to the 2-D restriction, flow (including turbulence) in the axial direction of the cylinder is suppressed.

Figure 10 shows the drag and lift coefficients on the primary cylinder at $\mathrm{Re} = 3000$, a gap spacing of 1·2, and three angles of attack: 15, 20, and 25°. At 20°, the lift coefficient on the primary cylinder is relatively flat, especially when compared to its behavior at the other two angles, and has a value just slightly greater than zero. At 15 and 25°, the lift coefficient has fairly irregular oscillations about a mean of slightly greater than zero. These results show that the configuration at 20° has the best behavior regarding lift reduction; vortex shedding from the primary cylinder is virtually suppressed due to the presence of the control cylinder. The time-averaged drag coefficient, also seen in Figure 10, for each of the three angles is about the same. At 15 and 25°, the instantaneous drag coefficient is somewhat irregular with a mean value of about 0·8. At 20°, the instantaneous drag coefficient is fairly flat with an average value of about 0.8. The average value for a single, isolated cylinder is about 0.95 at $\mathrm{Re} = 3000$. These results indicate that the presence of the control cylinder has a drag-reducing influence on the primary cylinder, with the best results obtained for 20°.

At $\mathrm{Re} = 3000$, the same behavior as at $\mathrm{Re} = 1000$ is noted regarding the wake length (although not shown). At the two angular placements (15 and 20°) of the control cylinder for which calculations were done, the 20° placement had the longer, hence steadier, wake which caused the lift coefficient to lessen and be reasonably steady. This is exactly the same behavior noted in Figures 8 and 9 for the $\mathrm{Re} = 1000$ case. At 20°, the wake extends farther downstream than at 15°. The wake at 20° shows a region of recirculation region in the center of the near-wake. The base pressure is affected by this recirculation in such a way that the drag and lift on the primary cylinder are both decreased with the lift having decreased significantly and with virtually no oscillation. The region of recirculation in the 20° wake plays the same role as a flexible splitter plate. In the 15° wake, there is no evidence of an organized recirculation and, consequently, the lift and drag both have an unsteadiness, albeit small, in this case not found in the 20° case.

Figure 11 shows the drag and lift coefficients for both cylinders at a gap spacing of 1·2 and two different angles of attack, 20 and 25°. As stated earlier, the control cylinder, being in the wake of the primary cylinder, does not see a steady approach velocity. The control cylinder, on the lower side of the upper shear layer, sees an irregular approach flow. The drag coefficient trace for the primary cylinder is reasonably flat at 20° with a value of about 0·75, while at 25° it has a small amplitude oscillation with approximately the same mean value. The value of 0·75 is a reduction from the single cylinder value of about 1·0 at $\mathrm{Re} = 3000$. The lift coefficient on the primary cylinder at 20° has a slight oscillation with a mean value of approximately 0·05 as compared to a single-cylinder value of $\pm 0{\cdot}35$ with a zero mean value. At 25°, the lift coefficient on the primary cylinder has an irregular behavior, with

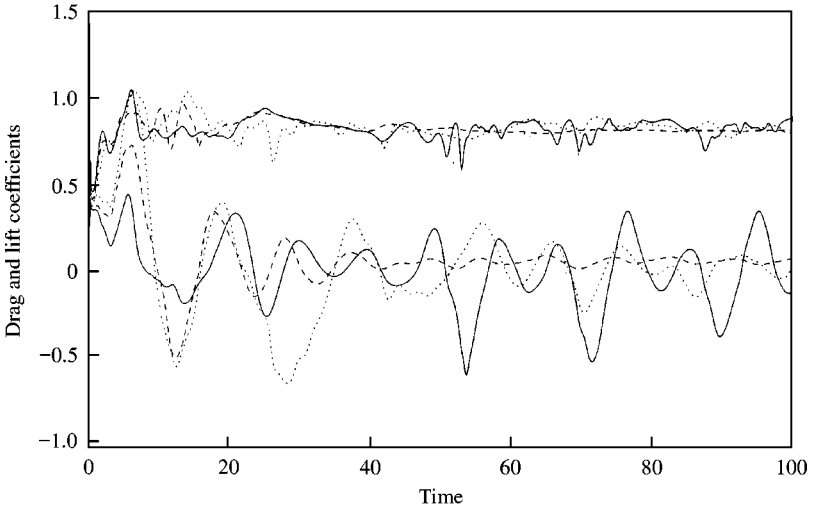

Figure 10. Drag and lift coefficients for the primary cylinder at Re = 3000 and $R/D = 1{\cdot}2$: ——, $\alpha = 15°$; – – –, $\alpha = 20°$; ····, $\alpha = 25°$.

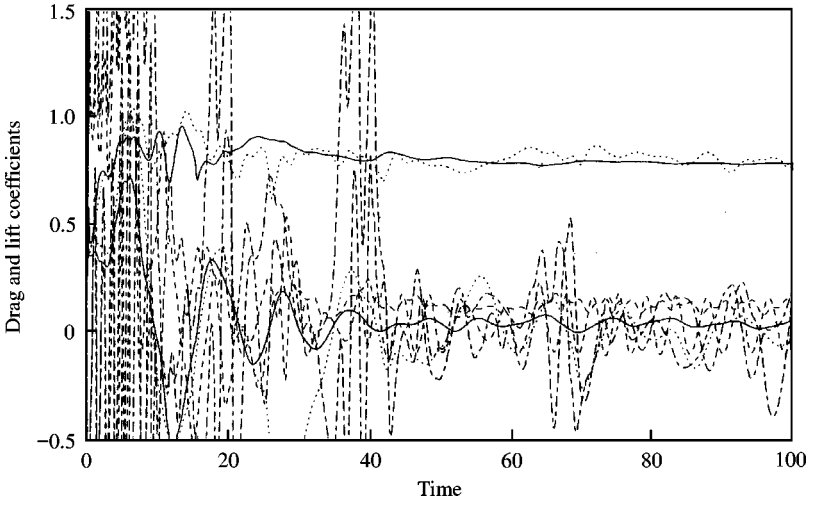

Figure 11. Drag and lift coefficients for both cylinders at Re = 3000, $R/D = 1{\cdot}2$, and $\alpha = 20°$, 25°. For $\alpha = 20°$: ——, primary; – – –, control. For $\alpha = 25°$; ····, primary; – – –, control.

evidence of an unidentified higher harmonic present in the signal, with a mean of approximately zero. The control cylinder at 20° has both drag and lift coefficients oscillating at small amplitude with approximately zero mean values while, at 25°, the lift and drag on the control cylinder each have a very irregular pattern with alternating regions of high and low amplitude behavior.

Figure 12 shows the contrast in the wake structures at Re = 3000, with and without the control cylinder in place, similar to Figure 9 for Re = 1000. For the Re = 3000 case, the control cylinder is at 20° and the gap spacing is 1·2. Again, the physical wake is 3-D and turbulent, making the flow visualization much less vivid than for a laminar flow case. However, the difference in the two wake structures is quite distinct. The pictures on the left,

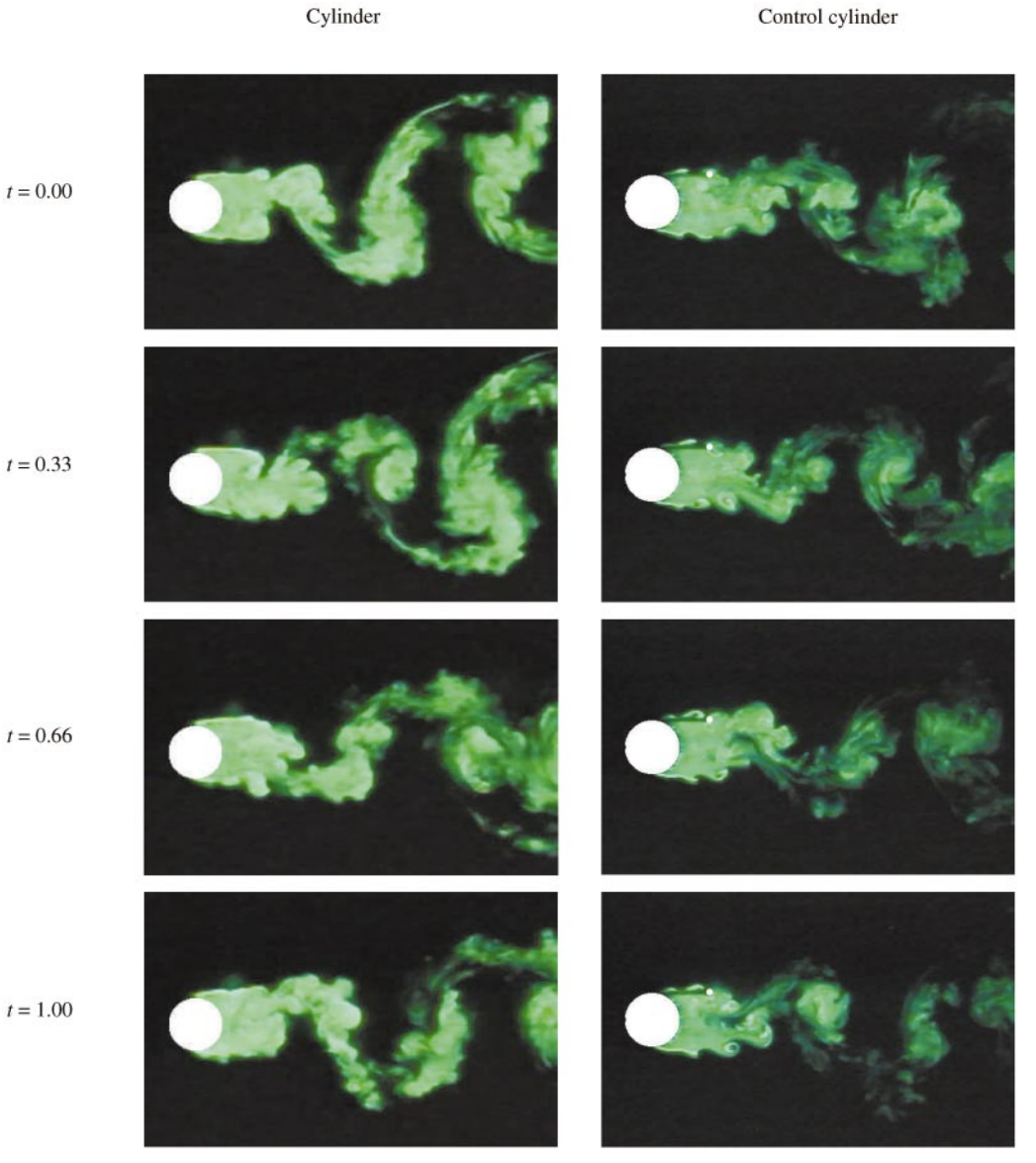

Figure 12. Flow visualization comparison at Re = 3000, $\alpha = 20^{\circ}$, and $R/D = 1{\cdot}2$.

without the control cylinder in place, show the classical alternate and periodic shedding of vortices, with the wake widening as the vortices move downstream. The pictures on the right, with the control cylinder in place, show a much narrower wake and a less pronounced vortex structure in the wake. The near-wake again seems to be less time-dependent, which is a result consistent with the calculated results.

5. CONCLUSIONS

We have shown that the presence of a properly placed small control cylinder in the wake of a primary cylinder can significantly reduce the possibility of vortex-induced vibration by

essentially eliminating conventional vortex shedding from the primary cylinder for $Re \leq 3000$. The suppression of conventional vortex shedding was found to be sensitive to both the angle of attack of the approach flow and the gap distance separating the centers of the two cylinders. The minimum values of both lift and drag on the primary cylinder were found to depend on both angle of attack and the gap distance. A physical application of this concept would have to be a flow which kept the same orientation to the primary and control cylinder, such as a flow past a pipeline spanning a river.

ACKNOWLEDGEMENTS

The authors are grateful to the University of Houston for the computer time used in these calculations. The second author is grateful to the State of Texas for his graduate support from the Advanced Technology Program on Grant no. 003652-019. The third author acknowledges EPSRC for his graduate support.

REFERENCES

IGARISHI, T. & TSUTSUI, T. 1991 Flow control around a circular cylinder by a new method (Third Report: Properties of the reattachment jet). *Proceedings JSME* **57,** 8–13 (in Japanese).

LU, X., DALTON, C. & ZHANG, J. 1997 Application of Large Eddy Simulation to flow past a circular cylinder. *ASME Journal of Offshore Mechanics and Arctic Engineering* **119,** 219–225.

SAKAMOTO, H., TAN, K., & HANUI, H. 1991 An optimum suppression of fluid forces by controlling a shear layer separated from a square prism. *ASME Journal of Fluids Engineering* **113,** 183–189.

SAKAMOTO, H. & HANUI, H. 1994 Optimum suppression of fluid forces acting on a circular cylinder. *ASME Journal of Fluids Engineering* **116,** 221–227.

SMAGORINSKY, J. 1963 General circulation experiments with the primitive equations. I. Basic experiments. *Monthly Weather Review* **91,** 99–164.

STRYKOWSKI, P. J. & SREENIVASAN, K. R. 1990 On the formation and suppression of vortex shedding at low Reynolds numbers. *Journal of Fluid Mechanics* **218,** 71–107.

ZDRAVKOVICH, M. M. 1997 *Flow Around Circular Cylinders. Volume 1: Fundamentals.* Oxford: Oxford University Press.